A WHITENING METHOD FOR THE DESPECKLING OF SAR IMAGES AFFECTED BY CORRELATED SPECKLE NOISE

Alessandro Lapini, Tiziano Bianchi, Fabrizio Argenti, and Luciano Alparone

Dipartimento di Elettronica e Telecomunicazioni – University of Florence
Via di Santa Marta, 3 – 50139 - Firenze - Italy
E-mail: {alessandro.lapini,tiziano.bianchi,fabrizio.argenti}@unifi.it, alparone@iapp.unifi.it

ABSTRACT

In the last decade, several methods have been developed for the despeckling of Synthetically Aperture Radar (SAR) images. A considerable number of them have been derived on the assumption of the fully–developed speckle model in which the multiplicative speckle noise is supposed to be a white process. Unfortunately, the transfer function of SAR acquisition systems can introduce a statistical correlation which decreases the despeckling efficiency of such filters.

In this work, a method for whitening a complex image acquired by a SAR system is proposed. By using the statistical properties of the acquired image the estimation of the SAR system frequency response is performed by means of some realistic assumptions; then a decorrelation process is applied on the acquired image, taking into account the presence of point targets. Finally, the image is despeckled. The experimental results show that the despeckling filters achieve better performance when they are preceded by the proposed whitening method; moreover, the radiometric characteristics of the image are preserved.

Index Terms— Despeckling, SAR images, whitening, correlated speckle noise, COSMO–SkyMed

1. INTRODUCTION

Speckle removal is a major problem in the analysis of SAR images. Speckle noise is a granular disturbance that affects the observed reflectivity. Usually, it is modelled as a multiplicative noise: this nonlinear behaviour makes the process of original information retrieval a nontrivial task [1]-[3]. In the recent years, multiresolution analysis tools have been successfully applied to the above problem [4]-[6]. Despeckling can be seen as an estimation problem. As such, the proposed statistical despeckling methods can be classified according to the estimation criterion and to the models of the processes that are involved. Bayesian methods, such as LMSSE and MAP criteria, have been taken into consideration both in the spatial and in the wavelet domain, e.g., in [1][2][5][6].

Most of the methods that have been proposed assume that the speckle noise is an uncorrelated process that affects the noise-free data. However, such a hypothesis does not often hold in practice. For example, the data acquired by the COSMO-SkyMed constellation of satellites demonstrate a strong correlation of the speckle. Using classical despeckling filters for such class of data yields unsatisfactory results. Few papers, e.g., [7], deals with the problem of restoring SAR images affected by correlated noise. Such processing needs an accurate statistical modeling of the acquired data, as can be found in [8].

In this paper, we propose a whitening algorithm that allows us to produce data that can be suitably processed with despeckling filters designed for uncorrelated speckle noise. This study, based on the results in [8] in order to estimate the SAR system transfer function, demonstrates that the whitening process is actually effective and allows classical despeckling filters to be fully exploited also for correlated speckle noise data. The experimental results, on synthetically speckled images and on true COSMO-SkyMed images, quantify the performance gain introduced by the proposed whitening approach.

2. SUB–OPTIMAL DESPECKLING PROBLEM

In [8], the spectral properties of a complex SAR images have been investigated and a generalization of the fully–developed speckle model has been given. Assuming the observed scene be composed by a set of point scatterers, let $\sigma_c(\mathbf{r})$ be the discrete complex backscatter coefficient per area that describes the radar target scene for each 2–D Cartesian coordinates $\mathbf{r} = (r_x; r_y)$. In the hypothesis of fully–developed speckle, σ_c is modeled as a white complex circular symmetric Gaussian process, having zero mean and variance $\sigma(\mathbf{r})$, where σ is the radar backscatter or *target scene*. By supposing that the entire acquisition chain is likely represented by a cascade of linear filters, we can synthesize them as the SAR system transfer function h. Using the previous assumptions, the complex

This study has been carried out under the financial support of Italian Space Agency (ASI), COSMO-SkyMed Scientific Projects, under contract I/043/09/0.

radar image g, i.e. the coherently acquired image, can be defined as

$$g(\mathbf{r}) = \mathfrak{F}^{-1}\left\{\Sigma_c(\mathbf{f}) \cdot H(\mathbf{f})\right\}, \tag{1}$$

where $\mathfrak{F}^{-1}\{\cdot\}$ denotes the inverse Fourier transform operator, Σ_c denotes the Fourier transform of σ_c and H is the Fourier transform of h. Hence, the despeckling problem consists in finding the estimator of the non-stationary radar backscatter σ given the observation of g. Although its general validity, the model expressed in (1) requires the explicit knowledge of the SAR system frequency response H.

The most used approach to the despeckling problem in the literature is based on the multiplicative speckle model:

$$|g(\mathbf{r})|^2 = \sigma(\mathbf{r}) \cdot sn(\mathbf{r}), \tag{2}$$

where sn is a multiplicative noise process that is supposed to be statistically independent of σ. Only in the very particular situation in which the SAR system transfer function is negligible, i.e. $g = \sigma_c$, the well known fully–developed speckle model is obtained:

$$|\sigma_c(\mathbf{r})|^2 = \sigma(\mathbf{r}) \cdot sn(\mathbf{r}), \tag{3}$$

where sn is modeled as a white random process having exponential distribution, with unitary mean and variance. However, in the general case the models given in (2) and in (1) are interchangeable only taking into account that sn is statistically correlated due to the SAR system frequency response. Despite this fact, most of the known despeckling filters are based on the hypothesis of uncorrelated speckle noise sn due to its simplicity.

In the proposed method, we follow a sub–optimal approach in order to solve the despeckling problem. We divide the main task in two consecutive steps:

1 *Whitening stage*: an estimator of the complex backscatter coefficients, $\hat{\sigma}_c$, is obtained from the complex image g using the general model given in (1).

2 *Despeckling stage*: the estimator of the radar backscatter, $\hat{\sigma}$, is finally obtained by using some known filter based on the model given in (3), where we replace σ_c with its estimator $\hat{\sigma}_c$.

As it has been pointed above, we are not directly interested in developing a new despeckling filter (what we called the *despeckling stage*) in this work. Instead, we focus our attention in developing an explicit expression for the estimator $\hat{\sigma}_c$ (*whitening stage*).

3. ESTIMATION OF THE COMPLEX BACKSCATTER COEFFICIENTS

The estimation of the source signal σ_c, given the observation of its output g from an unknown linear system h, is a typical problem of blind deconvolution. Several methods have been proposed in literature [9, 10] in the last two decades in the field of image restoration. Many of them are based on iterative algorithms and/or require some hypothesis on the prior distribution and the hyperparameters of the source signal, in order to use the Bayesian inference framework.

In our approach, any assumption on the statistical distribution of the target scene σ is avoided. Instead, we relax the problem doing some useful hypothesis on the SAR system. It is realistic to assume that the SAR system can be represented by a band-limited low-pass filter with cutoff frequency $\mathbf{f}_c$:

$$H(\mathbf{f}) \approx 0 \quad \forall |\mathbf{f}| > |\mathbf{f}_c|, \tag{4}$$

where $\mathbf{f}_c$ is known or it can be easily inferred by means of the observation of the spectrum of g. Then we define the estimator of the backscatter coefficients $\hat{\sigma}_c$ to be:

$$\hat{\sigma}_c(\mathbf{r}) = \begin{cases} \mathfrak{F}^{-1}\left\{G(\mathbf{f}) \cdot \left[\hat{H}(\mathbf{f})\right]^{-1}\right\} & \forall |\mathbf{f}| \le |\mathbf{f}_c|, \\ 0 & \text{otherwise.} \end{cases} \tag{5}$$

being $\hat{H}$ some estimator of H. Thus the blind deconvolution problem has been simplified in the estimation of the SAR system frequency response H. In the following discussion, a method for the estimation of H is presented.

3.1. Statistical property of the periodogram of the complex image

The average joint moment of the second order of g, taken over an $(2N_x + 1) \times (2N_y + 1)$ spatial grid $\mathbf{D}$, can be defined as

$$\overline{R_g}(\mathbf{r}) = \sum_{\mathbf{r}' \in \mathbf{D}} \frac{\mathrm{E}[g(\mathbf{r} + \mathbf{r}')g^*(\mathbf{r}')]}{(2N_x + 1)(2N_y + 1)}. \tag{6}$$

By supposing that a spatial average radar backscatter $\overline{\sigma}$ exists, and evaluating (6) when the dimensions of $\mathbf{D}$ tends to infinity, the average spectrum of g, $\overline{S}_g$, is obtained [8] as

$$\overline{S}_g(\mathbf{f}) = \mathfrak{F}\left\{\lim_{N_x \to +\infty} \lim_{N_y \to +\infty} \overline{R_g}(\mathbf{r})\right\} = \overline{\sigma}\,|H(\mathbf{f})|^2. \tag{7}$$

The average spectrum $\overline{S}_g$ can be estimated by means of the periodogram of g, $\hat{S}_g$ [7]:

$$\hat{S}_g(\mathbf{f}) = \frac{1}{N_c} \sum_{\mathbf{c} \in \mathbf{C}} \left| \mathfrak{F}\left\{g(\mathbf{r}) \cdot \frac{w(\mathbf{r} - \mathbf{c})}{N_w}\right\}\right|^2, \tag{8}$$

where $\mathbf{C}$ is an opportune subset of N_c points of the plane and w is a N_w–points window mask centered at $\mathbf{0}$. We define the estimation error of the periodogram $\hat{S}_g$, Δ_{S_g}, outside the SAR system stop-band, as

$$\Delta_{S_g}(\mathbf{f}) = \hat{S}_g(\mathbf{f}) - \overline{S}_g(\mathbf{f}) \qquad |\mathbf{f}| \leq |\mathbf{f}_c|. \tag{9}$$

Despite the fact that the statistical description of Δ_{S_g} involves the frequency components of the SAR system and it cannot be expressed in a closed form, some qualitative assessment can be derived. From the hypothesis given for the model in (1), it follows that the Fourier transform of g is a zero–mean white-noise complex circular symmetric Gaussian process [11]. By assuming that we deal with images whose dimensions are much larger than the distance at which the correlation is considerable, the subset $\mathbf{C}$ can be properly chosen such that the summation in (8) is computed over independent exponential random variables. Moreover, they can also be supposed equally distributed for a sufficiently large window w thanks to the ergodicity assumption on σ as stated in (7). Hence, according to the central limit theorem, the periodogram $\hat{S}_g$ converges in distribution to a Gaussian process having $\overline{S}_g$ mean and variance proportional to N_c^{-1} as N_c increases. Using the relation (9), the estimation error of the periodogram has probability distribution (pdf) given by

$$\text{pdf}_{\Delta_{S_g}(\mathbf{f})} \approx \mathcal{N}\left(0; \frac{\eta(\mathbf{f}, \overline{\sigma})}{N_c}\right) \quad \text{for} \quad N_c \to +\infty, \tag{10}$$

where η is some function which is independent from N_c. Since $\overline{S}_g$ depends upon the averaged radar backscatter $\overline{\sigma}$, the variance of $\Delta_{S_g}(\mathbf{f})$ is expected to be higher for brighter target scenes rather than for darker ones.

3.2. Estimation of the SAR system frequency response

It is reasonable that the SAR system transfer function h is a linear-phase FIR filter in order to avoid phase distortion in the detected image. In the following exposition we will do the slightly stronger hypothesis that the SAR system frequency response H is a real central–symmetric nonnegative function belonging to a set of parametrized curves $F(\boldsymbol{\theta})$, having known shape F and unitary energy, but unknown value of parameters vector $\boldsymbol{\theta} = (\theta_0, \ldots, \theta_{N_\theta - 1})$, N_θ finite . In symbols, it is expressed by:

$$\exists \boldsymbol{\theta} \in \Theta : H(\mathbf{f}) = F(\mathbf{f}; \boldsymbol{\theta}) \quad \forall \mathbf{f}, \tag{11}$$

such that, $\forall \mathbf{f}$ and $\forall \boldsymbol{\theta} \in \Theta$, we have

$$\begin{cases} F(\mathbf{f}; \boldsymbol{\theta}) \geq 0 \\ \exists \mathbf{f}_s(\boldsymbol{\theta}) : F(\mathbf{f} + \mathbf{f}_s; \boldsymbol{\theta}) = F(-\mathbf{f} + \mathbf{f}_s; \boldsymbol{\theta}) \\ \int_{|\mathbf{f}|<|\mathbf{f}_c|} F^2(\mathbf{f}; \boldsymbol{\theta}) \mathrm{d}\mathbf{f} = 1 \end{cases}, \tag{12}$$

where Θ is the parameters space. It should be noted that the hypothesis of unitary energy is needed to remove the gain ambiguity of the SAR system expressed in the model (1). Hence, we decide that our new goal is the indirect estimation of H by means of the direct estimation of the parameters vector $\boldsymbol{\theta}$, which fully defines the SAR system frequency response:

$$\hat{H}(\mathbf{f}) = F(\mathbf{f}; \hat{\boldsymbol{\theta}}). \tag{13}$$

Now, substituting (7) and (11) into (9), yields

$$\hat{S}_g(\mathbf{f}) = \overline{\sigma} F^2(\mathbf{f}; \boldsymbol{\theta}) + \Delta_{S_g}(\mathbf{f}). \tag{14}$$

We observed that Δ_{S_g} has zero mean and its energy is quite smaller than the averaged spectrum $\overline{S}_g$. Supposing to deal with ergodic processes, the average of the periodogram, $A_{\hat{S}_g}$, is:

$$\begin{aligned} A_{\hat{S}_g} &= \int \hat{S}_g(\mathbf{f}) \mathrm{d}\mathbf{f} = \int_{|\mathbf{f}|<|\mathbf{f}_c|} \left[\overline{\sigma} F^2(\mathbf{f}; \boldsymbol{\theta}) + \Delta_{S_g}(\mathbf{f})\right] \mathrm{d}\mathbf{f} \\ &\approx \overline{\sigma} \int_{|\mathbf{f}|<|\mathbf{f}_c|} F^2(\mathbf{f}; \boldsymbol{\theta}) \mathrm{d}\mathbf{f} + \int_{|\mathbf{f}|<|\mathbf{f}_c|} \mathrm{E}\left[\Delta_{S_g}(\mathbf{f})\right] \mathrm{d}\mathbf{f} \\ &\approx \overline{\sigma}, \end{aligned} \tag{15}$$

where we have substituted the relations (14) and (10) in the second and fourth step, respectively, and we have used the assumption of unitary energy given in (12). By using the definition given in (8) and extending the summation to the entire image, we can notice that the average energy of the complex image g, $\overline{E_g}$, is related to the average of periodogram:

$$\begin{aligned} A_{\hat{S}_g} &= \int \hat{S}_g(\mathbf{f}) \mathrm{d}\mathbf{f} \\ &= \frac{1}{N_c} \sum_{\mathbf{c} \in \mathbf{C}} \int_{|\mathbf{f}|<|\mathbf{f}_c|} \left|\mathfrak{F}\left\{g(\mathbf{r}) \cdot w(\mathbf{r} - \mathbf{c})\right\}\right|^2 \mathrm{d}\mathbf{f} \\ &= \frac{1}{N_c} \sum_{\mathbf{c} \in \mathbf{C}} \sum_{\mathbf{r}} \left| g(\mathbf{r}) \cdot \frac{w(\mathbf{r} - \mathbf{c})}{N_w} \right|^2 \\ &= \overline{E_g}, \end{aligned} \tag{16}$$

where the Parseval's theorem has been used in the second step. Hence we obtain from (16) and (15):

$$\overline{\sigma} \approx \overline{E_g}. \tag{17}$$

The relation in (17) can be now substituted into (14) in order to remove the dependency upon $\overline{\sigma}$:

$$\hat{S}_g(\mathbf{f}) = \overline{E_g} \cdot F^2(\mathbf{f}; \boldsymbol{\theta}) + \Delta_{S_g}(\mathbf{f}) \quad . \tag{18}$$

Following the model expressed in (18), the estimation of $\boldsymbol{\theta}$ can be accomplished by means of a model fitting which aims at minimizing the energy of Δ_{S_g}. In order to obtain a straightforward estimator of $\boldsymbol{\theta}$, we use a least squares approach. Thus, the least squares estimator of $\boldsymbol{\theta}$, $\hat{\boldsymbol{\theta}}_{\text{ls}}$, is given by

$$\hat{\boldsymbol{\theta}}_{\text{ls}} = \arg\min_{\boldsymbol{\theta}} \int_{|\mathbf{f}|<|\mathbf{f}_c|} \left|\Delta_{S_g}(\mathbf{f})\right|^2 \mathrm{d}\mathbf{f}, \tag{19}$$

where the quantity $\overline{E_g}$ is directly computed from g.

Finally, substituting (19) into (13), we obtain the estimator of the SAR system frequency response:

$$\hat{H}(\mathbf{f}) = F(\mathbf{f}; \hat{\boldsymbol{\theta}}_{\text{ls}}). \tag{20}$$

4. EXPERIMENTAL RESULTS

In this section, the experimental results obtained with the proposed method are presented. The GG–MAP–SEG filter [12] and the LMMSE filter [6] have been used to realize two different despeckling stages. For each of them, we have both implemented a version preceded by the whitening stage which we have introduced (shortly indicated with W–method) and a version without using it (indicated with N–method). Tests have been carried out on both synthetically generated speckled images and real SAR images.

4.1. Results on synthetically degraded images

A set of synthetically-speckled images have been generated according to (1), by using a 8 bit 512×512 test image (*Lena*) as target scene. The band-limited SAR system frequency response H has been supposed to be separable, i.e $H(\mathbf{f}) = H_x(f_x) \cdot H_y(f_y)$, with each component H_v, $v \in (x, y)$, belonging to the class of the raised cosine functions: $H_v(f) = A_v - B_v \cdot \cos[\pi(f + f_c)/f_c]$, $|f| \leq f_c$, where f_c is the known cutoff frequency and (A_v, B_v), $A_v > B_v > 0$, are the model parameters such that the filter has unitary energy. In order to avoid the results to be biased by a specific shape of the filter, the parameters (A_v, B_v) have been randomly generated for each realization of the complex images. Moreover, starting random values $(\tilde{A}_v, \tilde{B}_v)$ have been used to initialize the model fitting routine at each iteration.

The quality of each despeckled image has been measured by means of the peak SNR (PSNR), given by PSNR $= 10 \log 10(255^2/\text{MSE})$, where MSE is the mean square error between the filtered image and the original target scene, whose frequency components greater than the cutoff frequency f_c have been removed. Moreover, we have defined the PSNR gain $\Delta\text{PSNR} = PSNR_W - PSNR_N$, where $PSNR_W$ and $PSNR_N$ are respectively the PSNR obtained with the W–method and with the N–method.

Global statistics of the despeckling results have been computed for both methods, grouping them with respect to the simulated cutoff frequency f_c: the average PSNR obtained with the W–method ($\overline{\text{PSNR}}_W$), the average PSNR obtained with N–method ($\overline{\text{PSNR}}_N$) as well as the average and the standard deviation of the PSNR gain ($\overline{\Delta\text{PSNR}}$ and $\sigma_{\Delta\text{PSNR}}$, respectively). The obtained results are shown in Table 1. As can be seen, the W–method achieves a better despeckling performance for all the tested cutoff frequencies. The decrement of the averaged PSNR gain as f_c increases is consistent with the fact that when the noise tends to be uncorrelated the use of whitening becomes unnecessary. The better behavior in the absolute values of PSNR for the GG–MAP–SEG filter with respect to LMMSE is due to the intrinsic characteristics of the filters, with the former that generally surpasses the latter; however, the PSNR gain shows a similar decreasing trend.

4.2. Results obtained on real SAR images

As to the results on true SAR data, they have been assessed by using a 16 bit 2048×2048 single–look complex image, *Peretola*, representing the area of Florence airport and extracted from a 3–m resolution COSMO–SkyMed HImage Stripmap acquisition. In Figure 1, the original image and the despeckled versions obtained with the W–method and the N–method are shown. It can be observed that both methods behave similarly on textures and point targets, but the W–method considerably achieves better results on homogeneous areas. In order to compare the performance gap, the equivalent number of looks (ENL) has been computed over four homogeneous areas in the original and in the despeckled images; the results are reported in Table 2. Measurements confirm that the introduction of the whitening stage dramatically increases the effectiveness of the following despeckling stage.

Zone	original	N–method	W–method
1	1.00	23.89	114.94
2	1.01	18.24	137.08
3	1.03	22.58	86.30
4	0.92	16.56	89.69

Table 2. Comparison of the ENL obtained with the MAP–GG–SEG filter on four homogeneous areas.

5. CONCLUSIONS

Several known despeckling filters are developed on the hypothesis of white speckle noise; thus a performance penalty arises when they are applied to real SAR images, since SAR system can be usually modeled as a band-limited low-pass filter. In this paper, a whitening stage has been proposed to be applied before the despeckling stage. Furthermore, it has been derived only by means of the acquired image and some realistic assumptions on the SAR system frequency response; no hypothesis on the probability distribution of the radar backscatter has been done. The experimental results have been carried out on both synthetically degradated images and real SAR images. As the SAR system cutoff frequency moves away from the sampling frequency, it has been shown that an impressive improvement of despeckling performance is achieved by using the proposed method, with no evident loss in terms of texture and point targets preservation.

	LLMMSE				GG–MAP–SEG			
f_c	$\overline{\text{PSNR}}_N$	$\overline{\text{PSNR}}_W$	$\overline{\Delta\text{PSNR}}$	$\sigma_{\Delta\text{PSNR}}$	$\overline{\text{PSNR}}_N$	$\overline{\text{PSNR}}_W$	$\overline{\Delta\text{PSNR}}$	$\sigma_{\Delta\text{PSNR}}$
0.6	18.59	21.61	3.02	0.42	18.96	23.24	4.28	0.80
0.7	19.84	22.95	3.11	0.47	21.03	24.81	3.78	0.83
0.8	21.17	23.73	2.56	0.58	22.43	25.45	3.02	0.80
0.9	22.27	24.08	1.81	0.59	24.70	25.71	1.01	0.55

Table 1. PSNR obtained with the LMMSE and GG–MAP filters using different (normalized) cutoff frequencies.

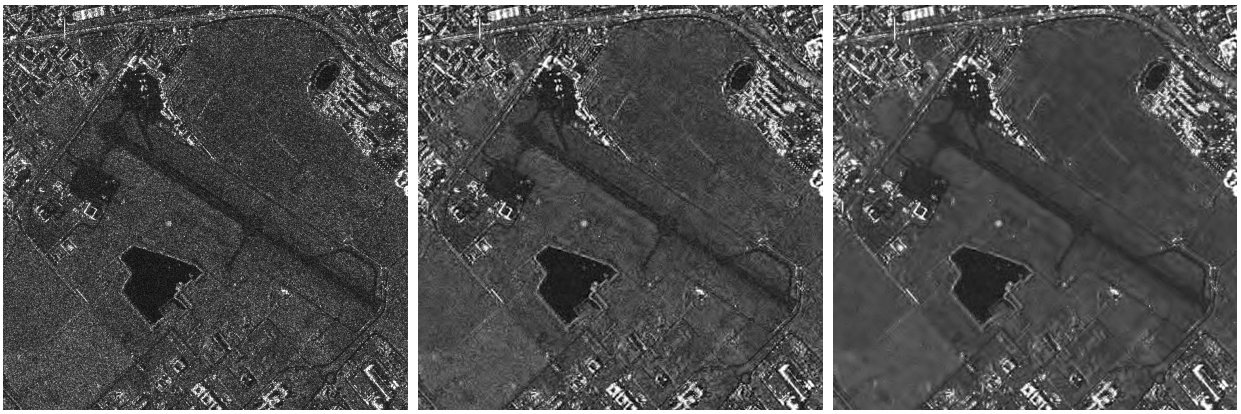

(a) (b) (c)

Fig. 1. Results obtained by processing a real SAR image. Left to right: original (a), N–method (b), W–method (c).

6. REFERENCES

[1] D. T. Kuan, A. A. Sawchuck, T. C. Strand, and P. Chavel, "Adaptive noise smoothing filter for images with signal-dependent noise," *IEEE Trans. on Pattern Anal. and Mach. Intell.*, vol. PAMI-7, no. 2, pp. 165–177, Feb. 1985.

[2] A. Lopes, R. Touzi, and E. Nezry, "Structure detection and statistical adaptive speckle filtering in SAR images," *International Journal of Remote Sensing*, vol. 14, no. 9, pp. 1735–1758, 1993.

[3] R. Touzi, "A Review of Speckle Filtering in the Context of Estimation Theory," *IEEE Trans. on Geosci. and Remote Sens.*, vol. 40, no. 11, pp. 2392–2404, Nov. 2002.

[4] A. Achim, P. Tsakalides, and A. Bezerianos, "SAR image denoising via Bayesian wavelet shrinkage based on heavy-tailed modeling," *IEEE Trans. on Geosci. and Remote Sens.*, vol. 41, no. 8, pp. 1773–1784, Aug. 2003.

[5] S. Foucher, G. B. Bénié, and J.-M. Boucher, "Multiscale MAP filtering of SAR images," *IEEE Trans. on Image Proc.*, vol. 10, no. 1, pp. 1019–1036, Jan. 2001.

[6] F. Argenti and L. Alparone, "Speckle removal from SAR images in the undecimated wavelet domain," *IEEE Trans. on Geosci. and Remote Sens.*, vol. 40, no. 11, pp. 2363–2374, Nov. 2002.

[7] S. Solbøand T. Eltoft, "A stationary wavelet-domain wiener filter for correlated speckle," *IEEE Transactions on Geoscience and Remote Sensing*, vol. 46, no. 4, pp. 1219–1230, Apr. 2008.

[8] S.N. Madsen, "Spectral properties of homogeneous and nonhomogeneous radar images," *Aerospace and Electronic Systems, IEEE Transactions on*, vol. AES-23, no. 4, pp. 583 –588, july 1987.

[9] D. Kundur and D. Hatzinakos, "Blind image deconvolution revisited," *IEEE Signal Processing Magazine*, vol. 13, no. 6, pp. 61 – 63, Nov. 1996.

[10] A. C. Likas and N. P. Galatsanos, "A variational approach for bayesian blind image deconvolution," *IEEE Transactions on Signal Processing*, vol. 52, no. 8, pp. 2222 – 2233, aug. 2004.

[11] F.D. Neeser and J.L. Massey, "Proper complex random processes with applications to information theory," *Information Theory, IEEE Transactions on*, vol. 39, no. 4, pp. 1293 –1302, jul 1993.

[12] T. Bianchi, F. Argenti, and L. Alparone, "Segmentation-based MAP despeckling of SAR images in the undecimated wavelet domain," *IEEE Trans. on Geosci. and Remote Sens.*, vol. 46, no. 9, pp. 2728–2742, Sept. 2008.